Chapter 3

Error Estimation

In this chapter we estimate the numerical error that was introduced by the spatial and angular discretization of the finite-difference discrete-ordinates method for solving the ERT. We performed calculations for different number of ordinates and different number of grid points.

3.1 Grid Size and Number of Ordinates

The finite-difference discrete-ordinates method as given in Chapter 2 is an approximation to the continuous ERT. The spatial derivatives of the ERT are approximated by finite differences, and the integral term (internal source term) of the ERT is replaced by a quadrature formula using discrete ordinates. These approximations introduce a numerical error, as a result of which the numerical solution differed somewhat from the analytical solution of the ERT. The magnitude of this numerical error depends on the number K of ordinates and on the number $I \times J$ of grid points. In this chapter we focus on the quantification of the errors that these approximations cause.

The impact of different numbers of ordinates and grid points on the numerical solution was determined by comparing the fluence profiles on the boundary of a test medium. We only compared relative fluence profiles, not absolute fluences. Therefore, the calculated fluences ϕ_{d} at the D detector positions were normalized by their mutual mean value[1]:

$$\phi_{\mathrm{d}}^{rel} = \frac{\phi_{\mathrm{d}}}{1/\mathrm{D}\sum_{\mathrm{d}}^{\mathrm{D}} \phi_{\mathrm{d}}}. \tag{3.1}$$

As explained later, relative fluence profiles could only be measured with our experimental set-up because the source strength was not exactly known (see Chapter 4). Furthermore, relative fluence profiles were always input to the MOBIIR scheme for reconstructing the optical parameters (see Chapters 7-9). Consequently, we were interested in determining the numerical error of relative fluence profiles instead of absolute fluence profiles.

First, we determined the impact of different numbers of ordinates in the forward calculation. A scattering medium with dimensions of 3 cm × 3 cm was used as a test example (see Figure 3.1). It had a scattering coefficient μ_s= 11.6 cm^{-1}, an absorption coefficient μ_a= 0.35 cm^{-1}, and an anisotropy factor $g = 0$. The light transport with non-reentry boundary conditions was solved on a grid with 181 × 181 grid points. We varied the number of ordinates with $\mathrm{K} \in \{4, 8, 12, 16, 32\}$. The isotropic source was positioned at one side of the medium with a distance of 0.3 cm to the adjacent boundary (source position A in Figure 3.1). The results are shown in Figure 3.2 for the fluence along the side opposite to the source position (x-axis), and along the side adjacent to the source position (y-axis). Provided that $\mathrm{K} > 4$, the number of ordinates had negligible impact on the numerical results for this particular test medium. However, it is well-known that for weakly-scattering media the *ray-effect* has a strong impact on the numerical results [Lathrop68] [Duderstadt79] [Chai93]. In these cases more ordinates have to be used.

Second, a similar numerical experiment was performed for an anisotropically scat-

[1]Note! D represents the number of detectors of one particular source. However, in Chapter 5 on page 70 we use D as the total number of all source-detector pairs.

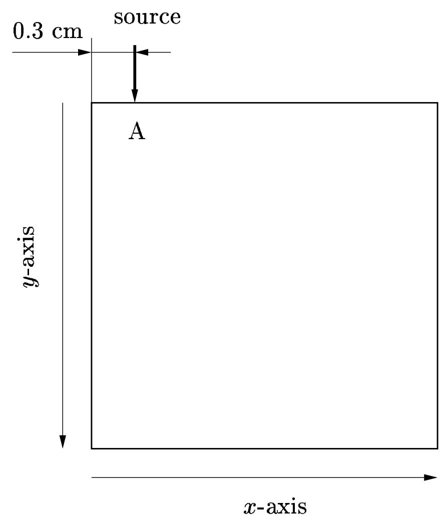

Figure 3.1: Schematic of the test medium with dimensions of 3 cm $\times$ 3 cm and source position A. The relative fluence profiles were taken on the boundary along the x-axis and y-axis.

tering medium with $g = 0.8$ and a scattering coefficient $\mu_s = 58$ cm^{-1}. As in the previous case, the reduced scattering coefficient was $\mu_s' = 11.6$ cm^{-1}. The results are shown in Figure 3.3. Again, the relative fluence profiles were almost independent of the number of ordinates for K > 4.

Additionally, we studied the impact of different grid sizes on the numerical result keeping the number of discrete ordinates constant (K=32). We chose 4 different grid sizes 31×31, 61×61, 181×181, and 361×361 with grid spacings $\Delta x = \Delta y$ of 0.1 cm, 0.05 cm, 0.01666 cm, and 0.00833 cm, respectively. For comparison, the isotropically scattering medium with $\mu_\mathrm{s} = 11.6$ cm^{-1} had a mean free pathlength of $1/\mu_\mathrm{s} = 0.0862$ cm, whereas the anisotropically scattering medium with $\mu_\mathrm{s} = 58$ cm^{-1} had a mean free pathlength of $1/\mu_\mathrm{s} = 0.01724$ cm.

In Figure 3.4 and in Figure 3.5 we show the fluence as a function of the spatial variable for different grid sizes of the isotropically and anisotropically scattering medium.

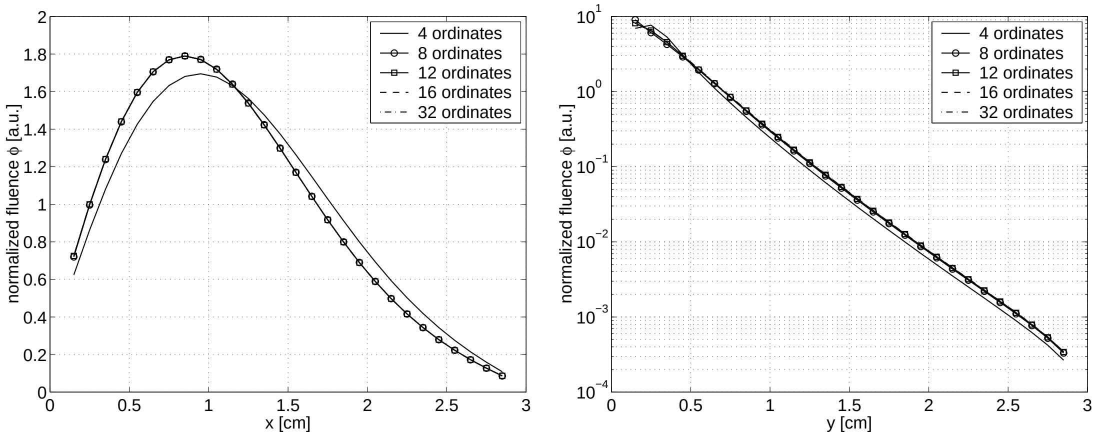

(a) Detector points along the x-axis.

(b) Detector points along the y-axis.

Figure 3.2: Relative fluence ϕ for different numbers of ordinates. The medium was isotropically scattering (g=0). The source was located at position A.

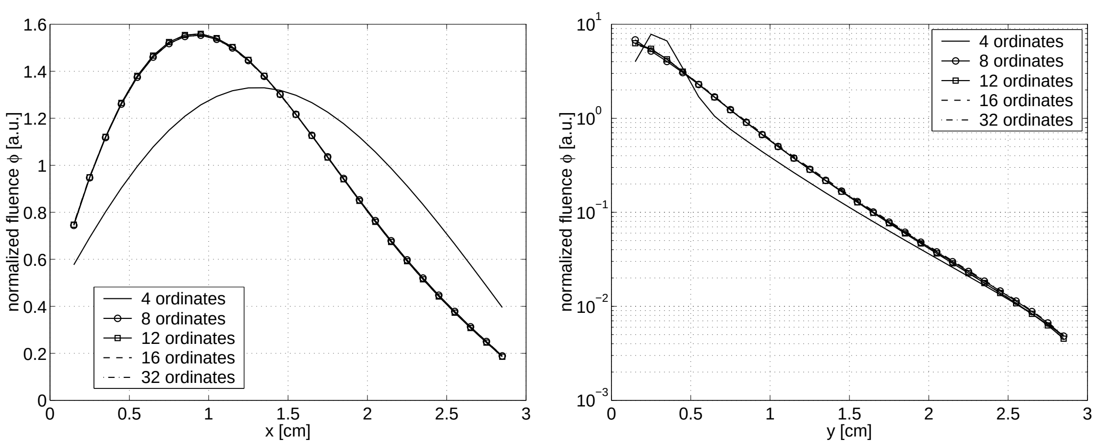

(a) Detectors along the x-axis.

(b) Detectors along the y-axis.

Figure 3.3: Relative fluence ϕ for different numbers of ordinates. The medium was anisotropically scattering (g=0.8). The source was located at position A.

As can be seen in Figures 3.4(a) and 3.5(a) the calculated fluence along the x-axis is only weakly dependent on the grid size. Differences between results obtained with a 31×31 grid and a 361×361 grid are smaller than 10%. Stronger differences are observed for data along the y-axis (Figures 3.4(b) and 3.5(b)). Especially at large distances from the sources the error accumulates and the results obtained with a 31×31 grid, are up to 5 times larger than the calculated fluences using a 361×361 grid.

The approximation of the spatial derivative by finite differences introduced a *truncation error*, which we called $\mathcal{O}$. The truncation error is quantified by using the *Taylor series expansion* at one grid point $a = (x_{\mathrm{i}}, y_{\mathrm{j}})$ along the x-axis. Expanding the Taylor series for the radiance $\psi(a + \Delta x)$ about a gives

$$\psi(a + \Delta x) = \psi(a) + \frac{\partial \psi(a)}{\partial a}\Delta x + \frac{\partial^2 \psi(a)}{\partial a^2}\Delta x^2 + \mathcal{O}(\Delta a^3). \tag{3.2}$$

We obtained an estimate for the first derivative by neglecting all higher terms on the right-hand side of Equation 3.2

$$\frac{\psi(a + \Delta x) - \psi(a)}{\Delta x} = \frac{\partial \psi(a)}{\partial a} + \mathcal{O}(\Delta x). \tag{3.3}$$

The upwind scheme, which uses the expression on the left-hand side of Equation 3.3, provides a first-order approximation to the first derivative with the truncation error $\mathcal{O}(\Delta x)$. This error is linearly dependent on the step size Δx for adjacent grid points. Therefore, the grid spacing Δx for a given medium has an effect on the computed radiance ψ that is proportional to Δx. If we decrease Δx, the numerical error $\mathcal{O}(\Delta x)$ decreases linearly. The same holds for Δy.

3.2 Discussion

We estimated the numerical error that was introduced due to the finite-difference discrete-ordinates method. We found that the numerical result did not strongly depend on

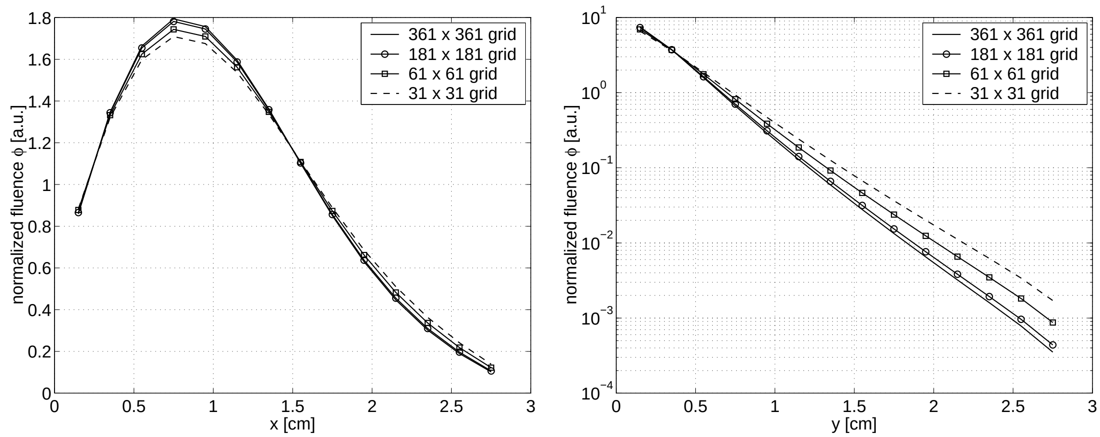

(a) Detectors along the x-axis. (b) Detectors along the y-axis.

Figure 3.4: Relative fluence ϕ for different numbers of grid points. The medium was isotropically scattering (g=0) and had optical parameters $\mu_s = 11.6\ \text{cm}^{-1}$ and $\mu_a = 0.35\ \text{cm}^{-1}$. The source was located at position A.

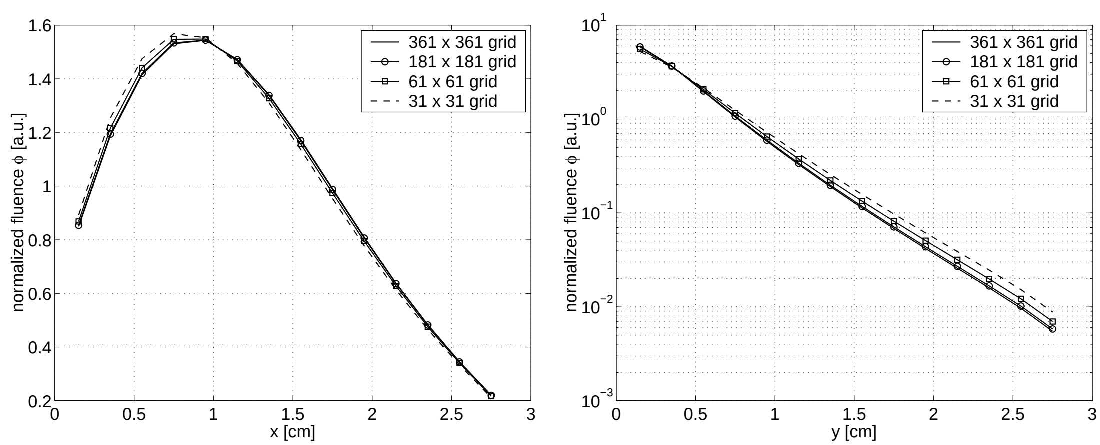

(a) Detectors along the x-axis. (b) Detectors along the y-axis.

Figure 3.5: Relative fluence ϕ for different numbers of grid points. The medium was anisotropically scattering ($g = 0.8$) and had optical parameters $\mu_s = 58\ \text{cm}^{-1}$ and $\mu_a = 0.35\ \text{cm}^{-1}$. The source was located at position A.

the degree of angular discretization for both the isotropically ($g = 0$) and anisotropically scattering medium ($g = 0.8$), when more than 4 ordinates were used. Similar results for the relative fluence profiles were obtained for 8,12,16, and 32 discrete ordinates. Therefore, we suggest for subsequent simulations to use at least $\mathrm{K} \geq 8$ discrete ordinates.

Varying the number of grid points used in the spatial discretization we found that a finer mesh yields more accurate solutions. We observed that the disparity between the different fluence profiles was larger along the y-axis than along the x-axis. This can be seen if we compare Figure 3.4(a) with Figure 3.4(b) for $g = 0$, or Figure 3.5(a) with Figure 3.5(b) for $g = 0.8$. Consequently, the use of detectors along the y-axis requires a finer discretization for calculating the fluence than the use of detectors along the x-axis opposite to the source.

Furthermore, we found for the isotropically scattering medium that at least a grid size of 181×181 grid points needed to be employed (see Figure 3.4(b)). This results in a grid spacing $\Delta x = \Delta y$ of 0.01666 cm between two grid points, which is approximately 1/5 of the mean free pathlength $1/\mu_{\mathrm{s}} = 0.0862$ cm of the scattering medium.

The anisotropically scattering medium ($g = 0.8$) with a mean free pathlength of $1/\mu_{\mathrm{s}} = 0.01724$ cm required only a grid spacing of 0.05 cm or 61×61 grid points, respectively (see Figure 3.5(b)). When we use the reduced scattering coefficient $\mu_{\mathrm{s}}' = (1 - \mathrm{g})\mu_{\mathrm{s}} = 11.6\ \mathrm{cm}^{-1}$ instead of μ_s, the step size between adjacent grid points had to be at least the mean free pathlength $1/\mu_{\mathrm{s}}' = 0.0862$ cm. This result is very encouraging for applications in tissue optics, where we encounter anisotropically scattering media with $g \geq 0.7$.

It was reported in the literature that the upwind scheme introduces an additional numerical error, called *numerical diffusion*, due to the first-order discretization of the spatial derivatives [Sewell88] [Fletcher90] [Chai93] [Mezzacappa99]. This artificial diffusion term, which is not present if higher-order discretization schemes are used, increases the fluence within the scattering medium. In order to match our numerical results with an analytical solution of the ERT or with experimental data we would have to increase the absorption coefficient within the upwind-difference discrete-ordinates method. This leads to the consequence that the upwind-difference scheme overestimates the absorption when employed within a MOBIIR scheme for reconstructing optical parameters.